Rhodobacter capsulatus 1-Deoxy-D-xylulose 5-Phosphate Synthase: Steady-State Kinetics and Substrate Binding†

Lisa M. Eubanks and C. Dale Poulter*

Department of Chemistry, University of Utah, Salt Lake City, Utah 84112

Received August 14, 2002; Revised Manuscript Received November 15, 2002

ABSTRACT: 1-Deoxy-D-xylulose 5-phosphate synthase (DXP synthase) catalyzes the thiamine diphosphate (TPP)-dependent condensation of pyruvate and D-glyceraldehyde 3-phosphate (GAP) to yield DXP in the first step of the methylerythritol phosphate pathway for isoprenoid biosynthesis. Steady-state kinetic constants for DXP synthase calculated from the initial velocities measured at varying concentrations of substrates were as follows: $k_{cat} = 1.9 \pm 0.1\ s^{-1}$, $K_m^{GAP} = 0.068 \pm 0.001$ mM, and $K_m^{pyruvate} = 0.44 \pm 0.05$ mM for pyruvate and GAP; $k_{cat} = 1.7 \pm 0.1\ s^{-1}$, $K_m^{D\text{-glyceraldehyde}} = 33 \pm 3$ mM, and $K_m^{pyruvate} = 1.9 \pm 0.5$ mM for D-glyceraldehyde and pyruvate. β-Fluoropyruvate was investigated as a dead-end inhibitor for pyruvate. Double-reciprocal plots showed a competitive inhibition pattern with respect to pyruvate and noncompetitive inhibition with respect to GAP/D-glyceraldehyde. $^{14}CO_2$ trapping experiments demonstrated that the binding of both substrates (pyruvate and GAP/D-glyceraldehyde) is required for the formation of a catalytically competent enzyme−substrate complex. These results are consistent with an ordered mechanism for DXP synthase where pyruvate binds before GAP/D-glyceraldehyde.

Isoprenoid compounds comprise the largest, most structurally diverse class of natural products consisting of more than 35 000 individual members. They are found in all organisms studied to date and include many essential compounds, such as sterols, ubiquinones, prenylated proteins, chlorophylls, and dolichols (*1*). The mevalonate (MVA) pathway found in eukaryotes and archaea (*2*) was widely accepted as the universal route for isoprenoid biosynthesis, until Rohmer and co-workers provided evidence for a new independent route in bacteria (*3*, *4*). This discovery led to the elucidation of the methylerythritol phosphate (MEP)[1] pathway, now known to be present in many eubacteria, green algae, and plants (*5*, *6*). In the MEP pathway, the five carbons of the isoprenoid unit are derived from pyruvate and D-glyceraldehyde 3-phosphate (GAP) in contrast to three molecules of acetyl-coenzyme A via the MVA pathway. Pyruvate and GAP are condensed to yield 1-deoxy-D-xylulose 5-phosphate (DXP) (Scheme 1). Rearrangement and reduction of DXP afford 2-methylerythritol 4-phosphate (MEP), the first committed intermediate in the MEP pathway for biosynthesis of isoprenoids (*7*, *8*). In addition, the corresponding alcohol, 1-deoxy-D-xylulose (DXS), is a substrate for the first pathway-specific enzymes of vitamin B_6 and vitamin B_1 synthesis (*9*). In four sequential steps, MEP is conjugated with cytidine monophosphate (CMP) (*10*), the C2 hydroxyl group is phosphorylated (*11*), CMP is eliminated to form a 2,4-cyclic diphosphate (*12*), and the ring is opened in a two-electron reduction process to form 1-hydroxy-2-methyl-2(*E*)-butenyl 4-diphosphate (*13*). Isopentenyl diphosphate (IPP) and dimethylallyl diphosphate (DMAPP), the five-carbon isoprene building blocks, are both synthesized from this common intermediate (*14*).

The initial step of the MEP pathway, the condensation of pyruvate and GAP to form DXP, is catalyzed by DXP synthase. This enzyme has been cloned, overexpressed, and purified from *Escherichia coli* (*15*), *Capsicum annuum* (*16*), *Streptomyces* sp. strain CL190 (*17*), and *Rhodobacter capsulatus* (*18*). *R. capsulatus*, a purple non-sulfur bacterium, is unique because it contains two DXP synthase genes (*18*). Purified, recombinant DXP synthase from *Streptomyces* and *R. capsulatus* are homodimers with 70 and 68 kDa subunits, respectively (*17*, *18*). Both cofactors, thiamine diphosphate (TPP) and divalent cation (Mg^{2+} or Mn^{2+}), are required for optimal enzymatic activity (*17*, *18*). Recombinant sources of DXP synthase are able to utilize either GAP or D-glyceraldehyde as the cosubstrate with pyruvate, although GAP appears to be the physiological substrate (*8*). Steady-state kinetic constants, apparent K_m and V_{max} values, have also been reported in the literature (*16*−*18*).

DXP synthases represent a newly discovered subclass of TPP-dependent enzymes that combine characteristics of decarboxylases and transketolases (tkts). On the basis of these similarities and the overall reaction mechanism for tkt (*19*), a mechanism for DXP synthase can be proposed (Scheme 2) as follows: formation of the highly reactive TPP ylide, nucleophilic attack of the ylide on the donor substrate

† This work was supported by National Institutes of Health Grant GM25521. L.M.E. is an NIH Predoctoral Trainee (Grant GM08573).

* To whom correspondence should be addressed. Phone: (801) 581-6685. Fax: (801) 581-4391. E-mail: poulter@chemistry.utah.edu.

[1] Abbreviations: CMP, cytidine monophosphate; DHAP, dihydroxyacetone phosphate; DMAPP, dimethylallyl diphosphate; DTT, dithiothreitol; DXP, 1-deoxy-D-xylulose 5-phosphate; DXS, 1-deoxy-D-xylulose; GAP, D-glyceraldehyde 3-phosphate; IPP, isopentenyl diphosphate; ME, 2-methylerythritol; MEP, 2-methylerythritol 4-phosphate; rt, room temperature; SAP, shrimp alkaline phosphatase; TIM, triosephosphate isomerase; TLC, thin-layer chromatography; tkt, transketolase; TPP, thiamine diphosphate.

10.1021/bi0205303 CCC: $25.00
Published on Web 01/04/2003

Scheme 1 Methylerythritol Phosphate Pathway for Isoprenoid Biosynthesis

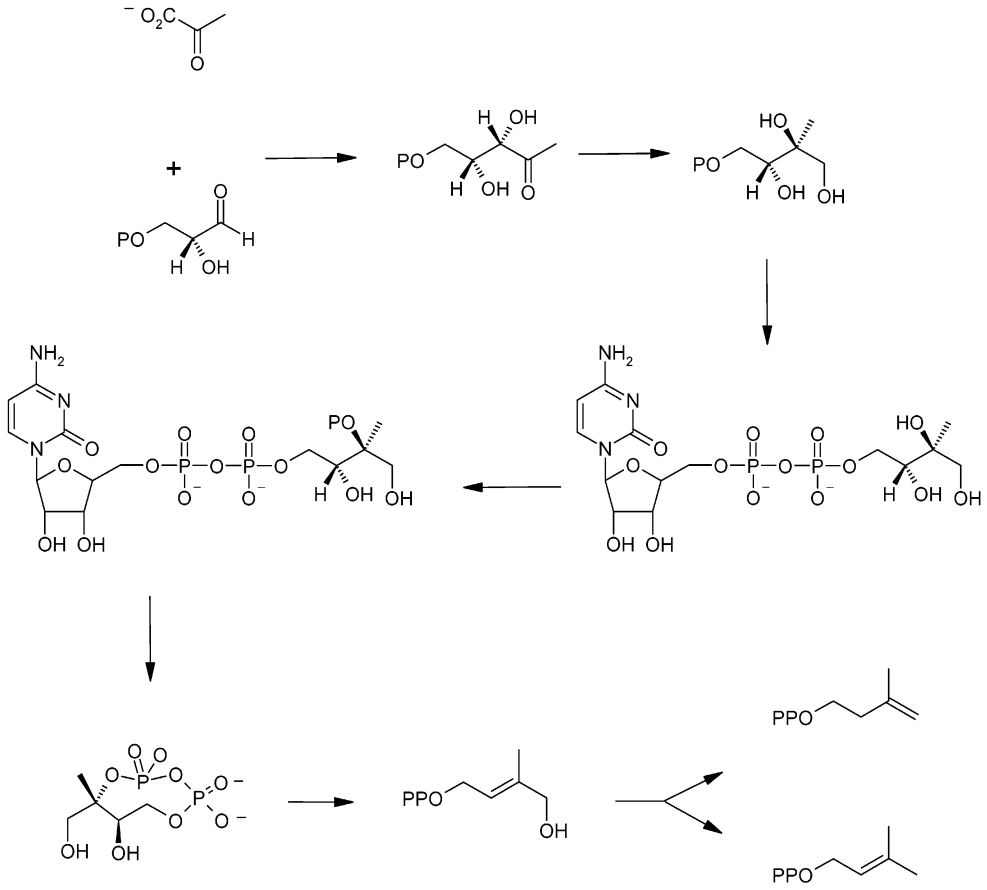

Scheme 2: Proposed Enzymatic Mechanism for DXP Synthase

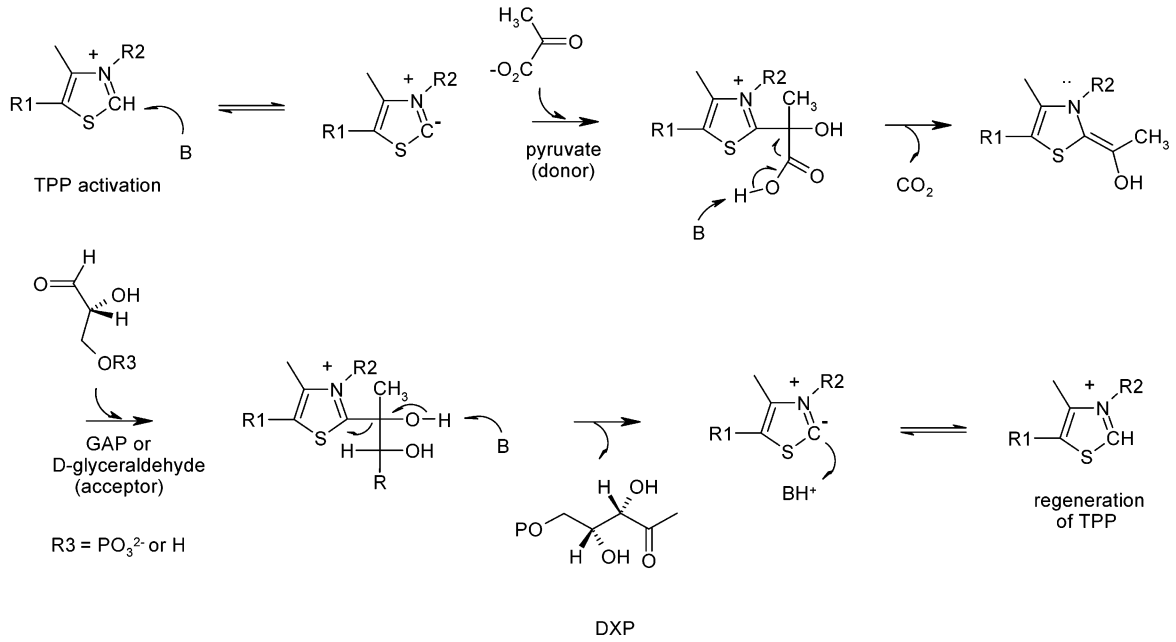

(pyruvate), elimination of the first product (CO_2), nucleophilic attack of the α-carbanion/enamine on the acceptor substrate (GAP or D-glyceraldehyde), elimination of the second product (DXP or DXS), and regeneration of TPP.

Like DXP synthase, two other TPP-dependent enzymes, acetolactate synthase and tkt, catalyze the condensation of a thiamine-bound two-carbon intermediate with a second substrate (Figure 1). The major difference among these enzymes is the donor and acceptor substrates utilized in the reaction. The donor and acceptor substrates for acetolactate synthase are both pyruvate. Tkt can catalyze the condensation of a variety of physiological substrates. However, the donor substrate is always a keto sugar, and the acceptor substrate is an aldo sugar. Detailed kinetic studies with acetolactate synthase and tkt have provided evidence for a ping-pong kinetic mechanism for these enzymes in which release of

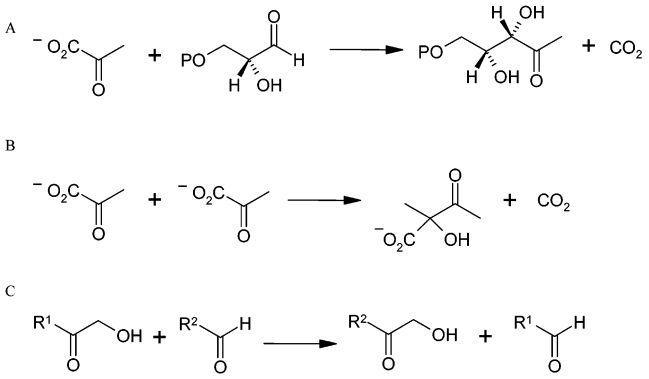

FIGURE 1: Reactions catalyzed by TPP-dependent enzymes: (A) DXP synthase, (B) acetolactate synthase, and (C) transketolase.

the first product precedes binding of the second substrate (*20*, *21*). Therefore, the question of whether this same type of mechanism is operative for DXP synthase arises.

The MEP pathway for isoprenoid biosynthesis provides a new target for antibacterial drugs and herbicides. Since DXP synthase catalyzes the first reaction in this pathway, a more thorough understanding of substrate binding and the kinetic mechanism of DXP synthase may aid in the design of more potent inhibitors. We now present steady-state kinetic studies, inhibition studies, and CO_2 trapping experiments that provide evidence for an ordered kinetic mechanism for DXP synthase where the binding of the second substrate (GAP or D-glyceraldehyde) is required for the formation of a catalytically competent enzyme−substrate complex.

EXPERIMENTAL PROCEDURES

Materials and General Methods. Sodium [2-^{14}C]pyruvate was purchased from Dupont New England Nuclear Research Products (Boston, MA). Triosephosphate isomerase (TIM), D-glyceraldehyde, dihydroxyacetone phosphate (DHAP), pyruvic acid, D-glyceraldehyde 3-phosphate (GAP), DL-α-glycerophosphate, β-glycerophosphate, 2,3-diphospho-D-glyceric acid, D-(−)-3-phosphoglyceric acid, and β-fluoropyruvic acid were purchased from Sigma (St. Louis, MO). Hydroxylamine hydrochloride, 2-carboxyethylphosphonic acid, and Dowex 1X8-200 ion exchange resin were purchased from Aldrich (Milwaukee, WI). Thiamine diphosphate (TPP) was purchased from ICN Biomedicals, Inc. (Costa Mesa, CA). Shrimp alkaline phosphatase (SAP) and sodium [1-^{14}C]pyruvate were from Amersham Pharmacia Biotech (Piscataway, NJ). Phosphonoacetohydroxamate was synthesized by the procedure of Cleland et al. (*22*). Recombinant *R. capsulatus* DXP synthase A was expressed in *E. coli* (pFMH30/BL21-DE3) and purified by ammonium sulfate precipitation and Ni^{2+}−silica affinity chromatography as described previously (*18*). Protein concentrations were measured by the method of Bradford (*23*). Pyruvate concentrations were determined using lactate dehydrogenase and NADH in an end point assay. Concentrations of DHAP were determined by phosphate analysis (*24*). Radioactivity was measured in Ultima Gold scintillation fluid from Packard (Meriden, CT) using a Packard Tri-Carb 2300TR liquid scintillation analyzer. Nuclear magnetic resonance spectra were acquired at 300 MHz. ^{31}P NMR spectra were referenced to external phosphoric acid (5%) in D_2O. Mass spectral data were collected by E. M. Rachlin on a thermo-Finnigan LCQ-classic (ion trap) electrospray mass spectrometer.

Phosphonopropionohydroxamate. Phosphonopropionohydroxamate was prepared essentially as described previously for phosphonoacetohydroxamate (*22*). 2-Carboxyethylphosphonic acid was first converted to the monoethyl ether followed by conversion to the hydroxamate (*22*). Phosphonopropionohydroxamate eluted from the Dowex 1X8-200 ion exchange column at 40 mM LiCl (*22*) and was obtained with an overall yield of 45%: ^{1}H NMR (D_2O) δ 1.48−1.62 (m, 2H), 2.18−2.3 (m, 2H); ^{13}C NMR (D_2O) δ 26.4 (d, J = 130.4 Hz), 29.5 (d, J = 3.0 Hz), 174.8 (d, J = 17.7 Hz); ^{31}P NMR (D_2O) δ 19.8 (s); MS-ES 168 (M − 1).

DXP Synthase Assays: Pyruvate and D-Glyceraldehyde. DXP synthase activity with pyruvate and D-glyceraldehyde as substrates was measured by incorporation of radioactivity into DXS from [2-^{14}C]pyruvate, as previously described (*18*). In all kinetic studies, reactions were carried out in duplicate at 37 °C in 200 mM sodium citrate (pH 7.4), 5 mM DTT, 2 mM $MgCl_2$, and 2 mM TPP in a final volume of 50 μL. Stock solutions of [2-^{14}C]pyruvate (0.42 μCi/μmol) and D-glyceraldehyde were diluted to the appropriate concentrations and added directly to the assay buffer. Assay mixtures were preincubated for 5 min at 37 °C and were initiated by the addition of enzyme (∼2.3 μg). After incubation at 37 °C for 15 min, the reactions were quenched by the addition of 50 μL of 0.5 M EDTA, and the mixtures were purified by silica chromatography (*18*). Radioactivity corresponding to [2-^{14}C]DXS was measured by liquid scintillation spectrometry. Control reaction mixtures for each concentration of pyruvate contained no DXP synthase and were subtracted as background.

DXP Synthase Assays: Pyruvate and D-Glyceraldehyde 3-Phosphate. DXP synthase activity with GAP as the cosubstrate was achieved using a coupled system as previously described (*18*). A constant supply of GAP for DXP synthase was generated in situ from DHAP and TIM. Assays contained 200 mM sodium citrate (pH 7.4), 5 mM DTT, 2 mM $MgCl_2$, 2 mM TPP, and TIM (5 units). Previously diluted solutions of [2-^{14}C]pyruvate (1.13 μCi/μmol) and DHAP were added, and the tubes were equilibrated at room temperature for 45 min. Assay mixtures containing TIM were preincubated for 5 min at 37 °C and the reactions initiated by adding enzyme (∼0.94 μg) to a final volume of 50 μL. Incubations were conducted at 37 °C for 3−17 min, followed by heating at 80 °C for 2 min. The $MgCl_2$ concentration was adjusted to 50 mM; 10 units of SAP was added, and the reaction mixture was incubated for an additional 90 min at 37 °C. The final enzymatic product was purified by silica chromatography, and the amount of radioactivity in [2-^{14}C]DXS was measured by liquid scintillation spectrometry. Initial velocities were determined from the slope of a plot of product versus time.

Inhibition Studies. Stock solutions of inhibitors were prepared in 200 mM sodium citrate (pH 7.4). Initial velocities were measured as specified above with minor modifications. Inhibition studies with β-fluoropyruvate were conducted with varying concentrations of inhibitor and substrate, either pyruvate, GAP, or D-glyceraldehyde. The appropriate cosubstrate was held constant at approximately K_m. The specific activity of pyruvate used for each study is listed within the figure legends.

The ability of DXP synthase to utilize β-fluoropyruvate as a substrate was examined by silica TLC. Reaction mixtures (50 μL) contained β-fluoropyruvate (20−60 mM), D-glyceraldehyde (30−100 mM), 200 mM sodium citrate (pH 7.4), 5 mM DTT, 2 mM $MgCl_2$, and 2 mM TPP. Reactions were initiated with 7.6 μg of affinity-purified enzyme. After 20−180 min at 37 °C, a 5 μL portion of the mixture was loaded onto a silica TLC plate. The plate was developed using a 1:3 methanol/$CHCl_3$ mixture and visualized with a *p*-anisaldehyde/sulfuric acid mixture (*25*). Control reactions were conducted with pyruvate (3−50 mM) and D-glyceraldehyde (30−100 mM).

Additional inhibition studies were performed with DL-α-glycerophosphate, β-glycerophosphate, 2,3-diphospho-D-glyceric acid, D-3-diphosphoglyceric acid, phosphonoacetohydroxamate, and phosphonopropionohydroxamate. Assays contained fixed unsaturating concentrations of pyruvate (2 mM, ∼0.12 μCi/μmol), 20 mM D-glyceraldehyde, and varying concentrations of inhibitor. The percent inhibition of DXP synthase was determined at the highest concentration of inhibitor experimentally possible.

Equations for Analysis of Kinetic Data. The initial velocities for DXP synthase measured at varying concentrations of pyruvate and GAP were fit to eq 1 using an explicit weighted nonlinear regression analysis (*26*), where [R] and [G] are the concentrations of pyruvate and GAP, respectively, K_{mR} and K_{mG} are the Michaelis constants for pyruvate and GAP at saturating second substrate concentrations, respectively, K_{ia} is the dissociation constant for pyruvate defined by the k_{-1}/k_1 ratio, ν is the velocity of product formation, and V_{max} is the maximal velocity of product formation.

$$\nu = \frac{V_{max}[R][G]}{K_{ia}K_{mR} + K_{mG}[R] + K_{mR}[G] + [R][G]} \quad (1)$$

The initial velocities for DXP synthase measured with varying concentrations of pyruvate and D-glyceraldehyde were fit to eq 2, which describes a case for substrate inhibition by D-glyceraldehyde, using an explicit weighted nonlinear regression analysis where both [G] and [I] is the concentration of D-glyceraldehyde and K_i is the substrate inhibition constant associated with D-glyceraldehyde binding to the free enzyme to give a dead-end complex.

$$\nu = \frac{V_{max}[R][G]}{K_{ia}K_{mG}(1 + [I]/K_i) + K_{mG}[R] + K_{mR}[G](1 + [I]/K_i) + [R][G]} \quad (2)$$

Data for inhibition studies in which β-fluoropyruvate and pyruvate were varied (fixed concentration of GAP or D-glyceraldehyde) were fit to eq 3 using an explicit weighted nonlinear regression analysis where [I] is the concentration of β-fluoropyruvate and K_i is the apparent inhibition constant associated with β-fluoropyruvate.

$$\nu = \frac{V_{max}[R]}{K_{mR}(1 + [I]/K_i) + [R]} \quad (3)$$

When GAP or D-glyceraldehyde was the varied substrate (fixed concentration of pyruvate), the inhibition constant for β-fluoropyruvate was determined from the replot of the intercepts versus inhibitor concentration. The simplified rate equation for noncompetitive inhibition by β-fluoropyruvate (eq 4) overestimates the change in slope and intercept under the experimental conditions.

$$\nu = \frac{V_{max}[G]}{K_{mG}(1 + [I]/K_i) + [G](1 + [I]/K_i)} \quad (4)$$

Therefore, it was necessary to determine the inhibition constant from the appropriate replot. The intercepts were obtained from the double-reciprocal plots of initial velocity versus the concentration of GAP or D-glyceraldehyde at fixed inhibitor concentrations. On the basis of the full rate equation for noncompetitive inhibition in an ordered kinetic mechanism (eq 2), the slope of the replot is defined in eq 5 where K_{mR} and V_{max} are determined from the steady-state kinetic studies.

$$\text{slope} = \frac{K_{mR}}{V_{max}[R]K_i} \quad (5)$$

CO_2 Trapping Studies. All assays contained a final sodium citrate concentration of 200 mM (pH 7.4) and 5 mM DTT. The amounts of TPP, $MgCl_2$, [1-^{14}C]pyruvate (0.71−2.93 μCi/μmol), and DXP synthase in the individual reactions are specified in the Results. The total amount of radioactivity per reaction was approximately 100 000 dpm. Moles of enzyme were calculated using the relationship in which 1 mol = 68 000 g of protein. This is based on the molecular mass for one subunit of DXP synthase [68 kDa (*18*)] and assumes that both subunits of the homodimer are active during catalysis. Assays were preincubated at 37 °C and initiated by the addition of enzyme (500 μL) in a final volume of 1 mL. $^{14}CO_2$ liberated during the course of the reaction was trapped with a 1.7 cm × 8.5 cm strip of Whatman #1 filter paper soaked in 0.2 mL of 1 M KOH (*27*). The reaction was quenched by addition of 1 mL of 2 M $HClO_4$ via syringe after 5−20 min at 37 °C. The reaction mixture was incubated for an additional 20 min at 37 °C to drive any remaining $^{14}CO_2$ out of the solution. The filter paper was transferred to a 20 mL scintillation vial containing 10 mL of Ultima Gold scintillation fluid. After vigorous vortexing had been carried out, the radioactivity corresponding to $^{14}CO_2$ was measured by liquid scintillation spectrometry within 1 h. The radioactivity remaining in the aqueous solution corresponding to [1-^{14}C]pyruvate was also measured to ensure efficient trapping. Control reactions were conducted under the same conditions but in the absence of enzyme and, therefore, served as a background for the assays.

Assays similar to those described above for the steady-state kinetic studies were also conducted. Reaction mixtures contained 200 mM sodium citrate (pH 7.4), 5 mM DTT, 2 mM $MgCl_2$, 2 mM TPP, 20 mM pyruvate (0.048 μCi/μmol), and 50 mM D-glyceraldehyde in a final volume of 50 μL. After preincubation for 5 min at 37 °C, the reaction was initiated by the addition of 15 μg (0.22 nmol) of enzyme. Incubation proceeded for 15 min at 37 °C, and the enzyme was precipitated by heating at 80 °C for 2 min. The rate of the reaction was determined from the loss of radioactivity in the assay mixture.

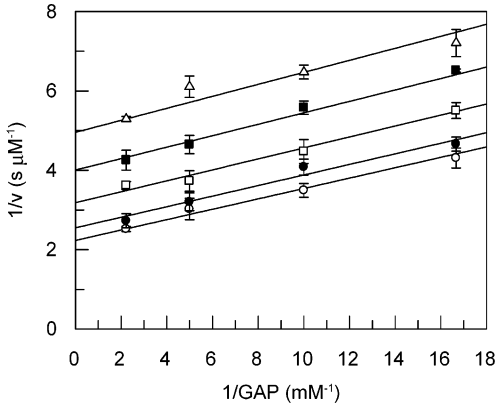

FIGURE 2: Double-reciprocal plot of initial velocities vs GAP concentrations at fixed concentrations of pyruvate. The concentration of GAP was varied between 0.06 and 0.45 mM at several pyruvate concentrations: 2.64 (○), 1.32 (●), 0.66 (□), 0.40 (■), and 0.28 mM (△). Reactions were conducted at 37 °C in buffer containing 200 mM sodium citrate (pH 7.4), 5 mM DTT, 2 mM $MgCl_2$, and 2 mM TPP.

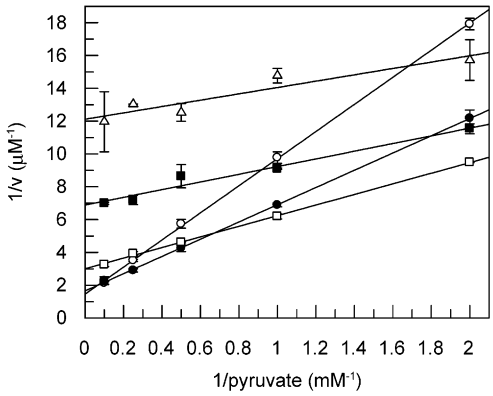

FIGURE 3: Double-reciprocal plot of initial velocities vs pyruvate concentrations at fixed concentrations of D-glyceraldehyde. The concentration of pyruvate was varied between 0.06 and 0.45 mM at several D-glyceraldehyde concentrations: 70.0 (○), 30.0 (●), 12.0 (□), 5.0 (■), and 2.5 mM (△). Reactions were conducted at 37 °C in buffer containing 200 mM sodium citrate (pH 7.4), 5 mM DTT, 2 mM $MgCl_2$, and 2 mM TPP.

RESULTS

Steady-State Kinetic Studies. Initial velocities for recombinant *R. capsulatus* DXP synthase A were measured using a discontinuous chromatographic assay that quantifies product formation by the incorporation of [2-^{14}C]pyruvate into product (*18*). Steady-state kinetic constants for DXP synthase with pyruvate and GAP as substrates were determined by fitting hyperbolic plots of initial velocity versus GAP concentration, at several fixed concentrations of pyruvate, to eq 1: $K_m^{GAP} = 0.068 \pm 0.001$ mM, $K_m^{pyruvate} = 0.44 \pm 0.05$ mM, $k_{cat} = 1.9 \pm 0.1$ s^{-1}, and $K_{ia} = 0.016 \pm 0.021$ mM. Double-reciprocal plots of the initial velocities versus the concentration of GAP, at different fixed concentrations of pyruvate, were essentially parallel over substrate concentrations between approximately $0.5K_m$ and $6K_m$ (Figure 2). This is consistent with a K_{ia} value that is very small compared to $K_m^{pyruvate}$, and therefore, the slopes of the plots are not affected by changes in pyruvate concentration (*28*). More specifically, the slopes of the plots of $1/v$ versus 1/[GAP] (Figure 2) are defined by eq 6.

$$\text{slope} = \frac{K_{mG}}{V_{max}}\left(1 + \frac{K_{ia}}{[R]}\right) \quad (6)$$

Under the experimental conditions, the calculated change in the slopes for each pyruvate concentration is <1%. This is in agreement with a similar plot of the raw data in which the actual change in slopes is also <1%. A similar trend is observed with the double-reciprocal plot of initial velocities versus pyruvate concentrations at fixed concentrations of GAP (data not shown).

Steady-state kinetic constants for DXP synthase with pyruvate and D-glyceraldehyde as substrates were determined by fitting hyperbolic plots of initial velocity versus pyruvate concentration, at several fixed concentrations of D-glyceraldehyde, to eq 2: $K_m^{D-glyceraldehyde} = 33 \pm 3$ mM, $K_m^{pyruvate} = 1.9 \pm 0.5$ mM, $k_{cat} = 1.7 \pm 0.1$ s^{-1}, $K_{ia} = 0.08 \pm 0.07$ mM, and $K_i = 15 \pm 4.0$ mM. Double-reciprocal plots of the initial velocities versus the concentration of pyruvate, at different fixed concentrations of D-glyceraldehyde, are shown in Figure 3. The competitive pattern observed at high concentrations of D-glyceraldehyde indicates that substrate inhibition results from addition of D-glyceraldehyde to the pyruvate binding site (*28*, *29*). Also, the plots of $1/v$ versus 1/[pyruvate] at fixed concentrations of D-glyceraldehyde show a nonlinear pattern that is most pronounced at high concentrations of D-glyceraldehyde and low concentrations of pyruvate (data not shown). This nonlinear pattern is indicative of substrate inhibition by D-glyceraldehyde.

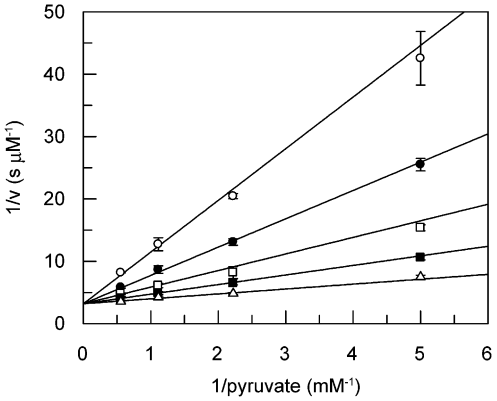

FIGURE 4: Inhibition of DXP synthase by β-fluoropyruvate. A double-reciprocal plot of initial velocities vs pyruvate concentrations (1.12 μCi/μmol) at 0.0 (△), 1.0 (■), 2.5 (□), 5.0 (●), and 10.0 mM (○) β-fluoropyruvate and a fixed unsaturating concentration of GAP (150 μM). Reactions were conducted at 37 °C in buffer containing 200 mM sodium citrate (pH 7.4), 5 mM DTT, 2 mM $MgCl_2$, and 2 mM TPP.

Kinetic Studies with Dead-End Inhibitors. β-Fluoropyruvate was used as a dead-end inhibitor for pyruvate to distinguish between a random and ordered binding mechanism for DXP synthase. A TLC assay was used to confirm that β-fluoropyruvate was an unreactive analogue of pyruvate. Double-reciprocal plots of the initial velocities for varied concentrations of pyruvate and unsaturating concentrations of GAP and D-glyceraldehyde at different fixed concentrations of β-fluoropyruvate are shown in Figures 4 and 5, respectively. When pyruvate was the varied substrate, in the presence of either GAP or D-glyceraldehyde, the data for inhibition by β-fluoropyruvate show a competitive inhibition pattern with K_i values of 1.0 ± 0.1 and 6.1 ± 0.3 mM, respectively.

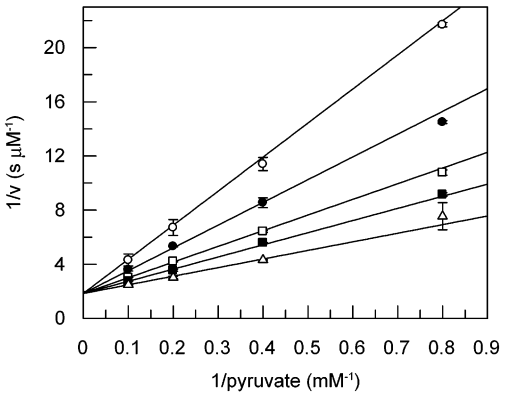

FIGURE 5: Inhibition of DXP synthase by β-fluoropyruvate. A double-reciprocal plot of initial velocities vs pyruvate concentrations (0.21 μCi/μmol) at 0.0 (△), 2.5 (■), 5.0 (□), 10.0 (●), and 18.0 mM (○) β-fluoropyruvate and a fixed unsaturating concentration of D-glyceraldehyde (35 mM). Reactions were conducted at 37 °C in buffer containing 200 mM sodium citrate (pH 7.4), 5 mM DTT, 2 mM $MgCl_2$, and 2 mM TPP.

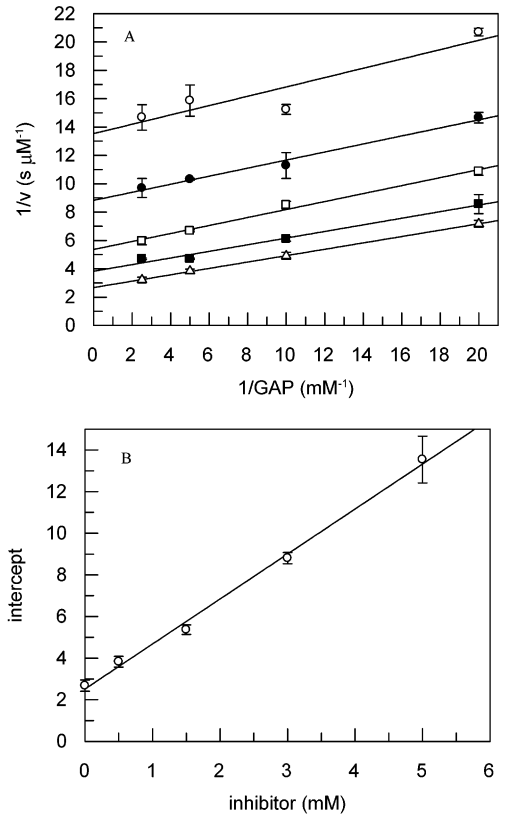

FIGURE 6: Inhibition of DXP synthase by β-fluoropyruvate. (A) Double-reciprocal plot of initial velocities vs GAP concentrations at 0.0 (△), 0.5 (■), 1.5 (□), 3.0 (●), and 5.0 mM (○) β-fluoropyruvate and a fixed unsaturating concentration of pyruvate (450 μM, 2.9 μCi/μmol). (B) Replot of intercepts vs the concentration of β-fluoropyruvate. Reactions were conducted at 37 °C in buffer containing 200 mM sodium citrate (pH 7.4), 5 mM DTT, 2 mM $MgCl_2$, and 2 mM TPP.

Double-reciprocal plots of the initial velocities for varied concentrations of GAP or D-glyceraldehyde at different fixed concentrations of β-fluoropyruvate are shown in Figure 6A and Figure 7A. Replots of the intercepts from the double-reciprocal plots versus β-fluoropyruvate concentrations are shown in Figures 6 and 7B. If the mechanism for DXP synthase is ordered, then the slope of the replots is defined

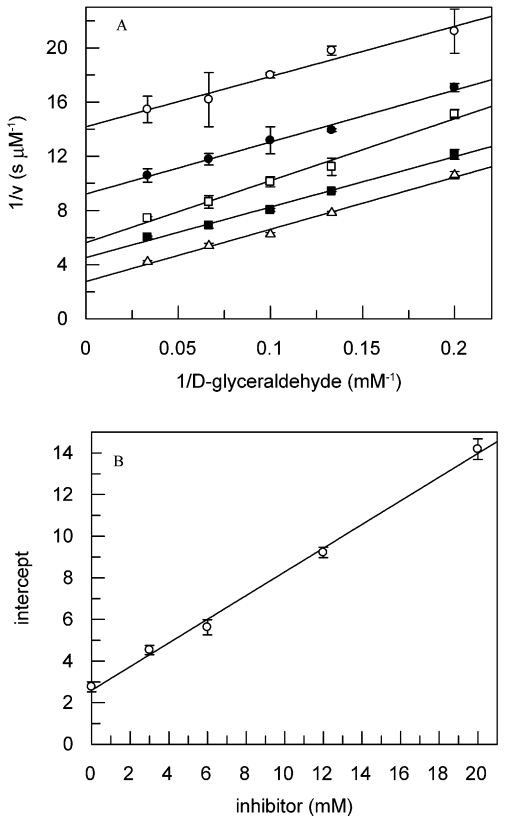

FIGURE 7: Inhibition of DXP synthase by β-fluoropyruvate. (A) Double-reciprocal plot of initial velocities vs D-glyceraldehyde concentrations of 0.0 (△), 3.0 (■), 6.0 (□), 12.0 (●), and 20.0 mM (○) β-fluoropyruvate and a fixed unsaturating concentration of pyruvate (3.0 mM, 0.42 μCi/μmol). (B) Replot of intercepts vs the concentration of β-fluoropyruvate. Reactions were conducted at 37 °C in buffer containing 200 mM sodium citrate (pH 7.4), 5 mM DTT, 2 mM $MgCl_2$, and 2 mM TPP.

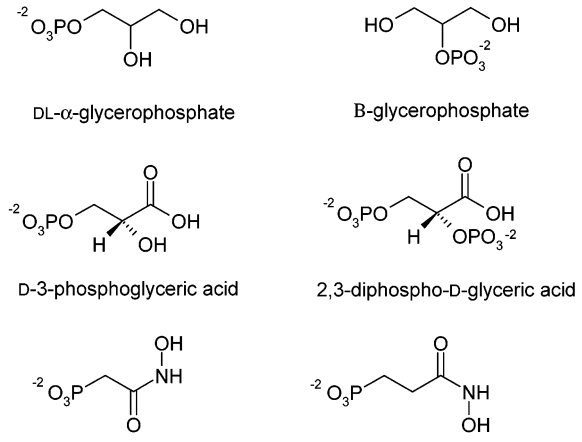

FIGURE 8: Structures of the compounds examined as inhibitors of DXP synthase.

by eq 5. Therefore, the inhibition constants determined using eq 5 and the previously determined values for K_{mR} and V_{max} (steady-state kinetic studies within) are 0.63 ± 0.07 and 2.0 ± 0.2 mM for varied GAP and D-glyceraldehyde concentrations, respectively.

Several compounds were screened as possible dead-end inhibitors for GAP/D-glyceraldehyde (Figure 8). DL-α-Glycerophosphate, β-glycerophosphate, 2,3-diphosphate-D-glyceric acid, and D-3-phosphoglyceric acid were investigated

Table 1: Compounds Examined as Inhibitors of DXP Synthase[a]

compound	concentration (mM)	% inhibition
DL-α-glycerophosphate	290	50
β-glycerophosphate	300	40
2,3-diphospho-D-glyceric acid	100	50
D-3-phosphoglyceric acid	160	23
phosphonoacetohydroxamate	100	25
phosphonopropionohydroxamate	100	10

[a] Assays contained 2 mM pyruvate (~0.12 μCi/μmol), 20 mM D-glyceraldehyde, and maximal concentrations of inhibitor. Reactions were conducted at 37 °C in buffer containing 200 mM sodium citrate (pH 7.4), 5 mM DTT, 2 mM $MgCl_2$, and 2 mM TPP.

as possible mimics for GAP. Phosphonoacetohydroxamate and phosphonopropionohydroxamate were examined as possible transition-state analogues. Unfortunately, none of these compounds were potent inhibitors of DXP synthase. The percent inhibition for each compound, determined at the highest concentration experimentally possible, is listed in Table 1.

CO_2 Trapping Studies. The small change in the slopes observed in the steady-state kinetic (Figures 2 and 3) and inhibition studies (Figures 6 and 7) is presumably due to a K_{ia} value that is very small compared to $K_m^{pyruvate}$. Although, these studies do not permit one to conclusively distinguish between an ordered mechanism and a ping-pong mechanism because a ping-pong mechanism predicts that these slopes will be constant. Therefore, the small changes observed and predicted (less than 10%) may be within experimental error. As a result, it was necessary to establish whether binding of the second substrate, GAP or D-glyceraldehyde, to DXP synthase is required for catalysis.

CO_2 trapping experiments were conducted with [1-^{14}C]-pyruvate so that the radioactivity corresponding to $^{14}CO_2$ release could be quantified by liquid scintillation spectrometry, as described in Experimental Procedures. Control reactions were conducted under conditions similar to those used for the steady-state kinetic studies to ensure that the rate of the reaction was not affected by the addition of [1-^{14}C]pyruvate, instead of [2-^{14}C]pyruvate. At low DXP synthase concentrations, compared to pyruvate and D-glyceraldehyde concentrations, the specific activity of DXP synthase was 1.4 μmol min^{-1} mg^{-1}. This is in agreement with a V_{max} of 1.6 μmol min^{-1} mg^{-1}, determined for the enzymatic reaction with pyruvate and D-glyceraldehyde as cosubstrates for DXP synthase.

The results of a series of experiments, along with the concentrations of DXP synthase, pyruvate, TPP, and Mg^{2+}, are listed in Table 2. The mixture for reaction 1 contained approximately stoichiometric amounts of enzyme, pyruvate, and cofactors. The percent conversion for this reaction was only 32% (Figure 9) with a rate of 0.16 nmol min^{-1} mg^{-1}. If DXP synthase catalyzes the conversion of pyruvate to the TPP−acetaldehyde complex and CO_2 in the absence of GAP or D-glyceraldehyde, the rate of the reaction should be >32 nmol min^{-1} mg^{-1} (the rate calculated for the formation of the final product, DXS or DXP). Also, the reaction should be 100% complete in 20 s. The observed rate is at least 200-fold lower than expected and the reaction only 32% complete after 20 min. A time course study under the conditions of reaction 1 was also conducted to ensure that the enzyme was stable over the course of 20 min. Samples of the enzyme

Table 2: Results of $^{14}CO_2$ Trapping Experiments

reaction	DXP synthase (nmol/μM)[a]	pyruvate (nmol/μM)[a]	TPP (nmol/μM)[a]	$MgCl_2$ (nmol/μM)[a]	% conversion[b]	rate[c] (nmol min^{-1} mg^{-1})
1	20	15	30	30	32	0.16
2	20	15	75	75	35	0.18
3	20	75	75	75	87	2.2
4	20	75	30	75	45	1.1

[a] The reaction volumes are 1 mL; therefore, the number of nanomoles is equivalent to the molarity of each component. [b] Percent conversion is calculated with the ratio of the radioactivity trapped vs the total amount of radioactivity per reaction. One mole of CO_2 is equal to 1 mol of decarboxylated pyruvate. [c] Specific activity for a 20 min reaction. Reactions were conducted at 37 °C in buffer containing 200 mM sodium citrate (pH 7.4), 5 mM DTT, and specified amounts of pyurvate, TPP, $MgCl_2$, and DXP synthase.

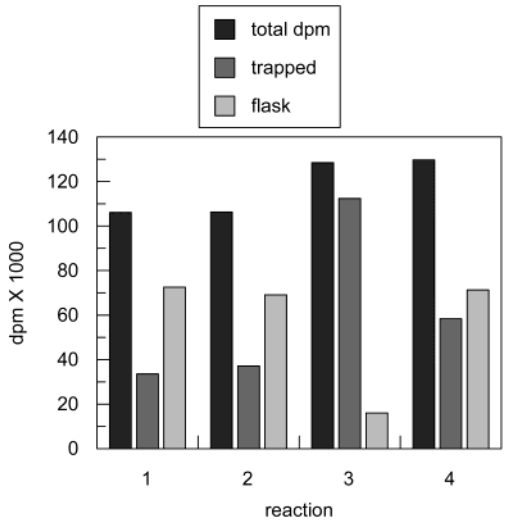

FIGURE 9: CO_2 trapping data for each reaction in Table 2. The total disintegrations per minute per reaction ([1-^{14}C]pyruvate), disintegrations per minute trapped ($^{14}CO_2$ liberated), and disintegrations per minute in solution after incubation with DXP synthase (unreacted [1-^{14}C]pyruvate) are illustrated.

taken at all of the time points displayed a rate of approximately 0.16 nmol min^{-1} mg^{-1}, demonstrating that the reaction was linear with time.

The mixture for reaction 2 contains approximately stoichiometric amounts of pyruvate and DXP synthase and elevated concentrations of TPP and $MgCl_2$. The percent conversion and observed rate are similar to those of reaction 1. Again, the observed rate is at least 200-fold lower than expected if DXP synthase catalyzed the decarboxylation of pyruvate in the absence of GAP or D-glyceraldehyde.

The mixture for reaction 3 contained increased amounts of pyruvate, TPP, and $MgCl_2$ with respect to DXP synthase. The percent conversion was 87% after 20 min (100% completion in 20 s is expected) with a rate of 2.2 nmol min^{-1} mg^{-1} (100-fold lower than expected). In this reaction, the amount of pyruvate that is decarboxylated is 3-fold higher than the amount of DXP synthase, suggesting multiple turnovers under these conditions. Perhaps in the absence of the second substrate but with excess pyruvate, a second molecule of pyruvate binds to the enzyme active site and promotes the first half of the catalytic cycle. Release of the TPP−acetaldehyde complex from the active site of DXP synthase would allow for additional binding of free TPP and

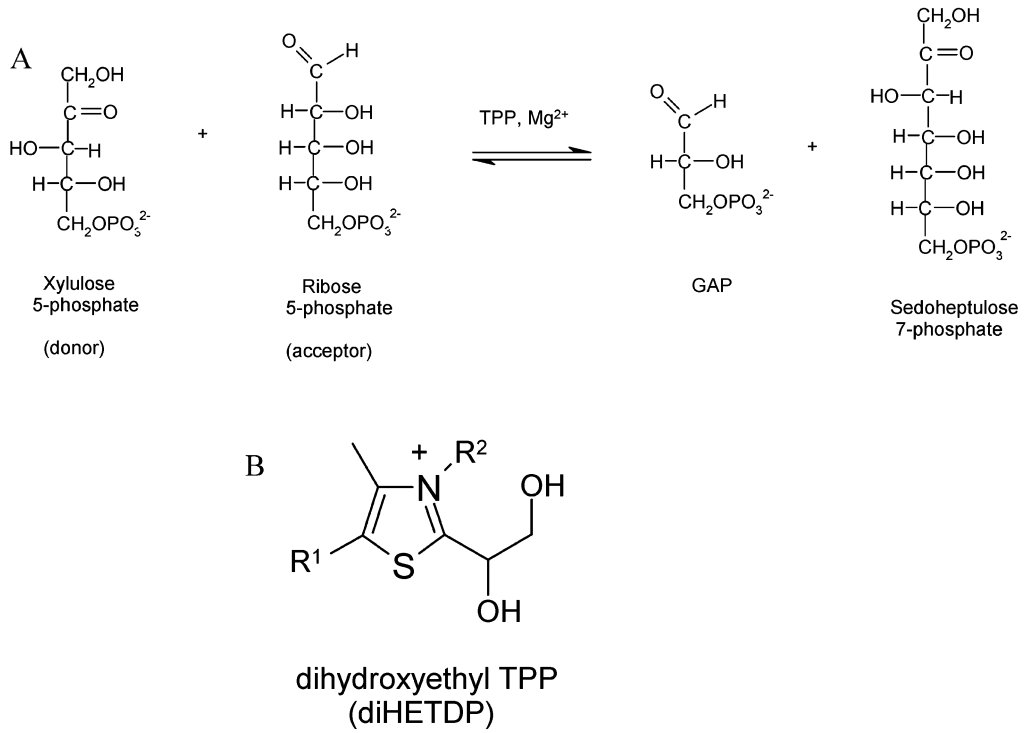

FIGURE 10: TPP-dependent enzyme transketolase. (A) Physiological enzymatic reaction of transketolase. (B) Chemical structure of dihydroxyethylthiamine diphosphate.

pyruvate and, ultimately, additional catalytic cycles. A slight increase in the reaction rate might result from the excess pyruvate binding to DXP synthase, although complete conversion of pyruvate to the TPP−acetaldehyde complex and CO_2 is still not observed.

The mixture for reaction 4 contained approximately stoichiometric amounts of TPP and DXP synthase, and elevated amounts of pyruvate and $MgCl_2$. The percent conversion was 45% after 20 min, corresponding to the decarboxylation of 33 nmol of pyruvate. It has been observed in tkt and other TPP-dependent enzymes that the TPP-bound two-carbon intermediate formed in the enzymatic reaction is stable. Therefore, the degradation of the TPP−acetaldehyde intermediate formed by DXP synthase to acetaldehyde and free TPP is not favorable.

One possible explanation for the results observed in reaction 4 might be that all of the TPP (30 nmol) is converted to the stable TPP−acetaldehyde form. This scenario requires an equal amount of pyruvate (30 nmol), similar to the actual amount of pyruvate that is decarboxylated. The decarboxylation of additional pyruvate would require more free TPP, the level of which has been depleted.

DISCUSSION

DXP synthase catalyzes the first step in the biosynthesis of isoprenoids and B vitamins via the MEP pathway. In the MEP pathway, pyruvate and GAP are condensed to form DXP. Recombinant DXP synthase can utilize either GAP or D-glyceraldehyde as the cosubstrate with pyruvate to form DXP or DXS, respectively. The first half-reaction catalyzed by DXP synthase involves the decarboxylation of pyruvate in forming a TPP-bound two-carbon intermediate and CO_2. Several other TPP-dependent enzymes, such as pyruvate decarboxylase and benzylformate decarboxylase, catalyze the decarboxylation of pyruvate and benzylformate, respectively, to form the appropriate decarboxylated product and CO_2. Even though this is similar to the first half-reaction of DXP synthase, the overall reaction of these enzymes does not entail the transfer of the two-carbon unit to a second substrate. Therefore, the overall reaction of DXP synthase and its kinetic mechanism are best compared to those of tkt and acetolactate synthase.

It has been widely accepted that tkt proceeds through a classical ping-pong mechanism where tkt binds the first substrate, catalyzes the formation of a stable TPP-bound two-carbon intermediate, and releases the first product before binding the second substrate. One of the physiological reactions of tkt with xylulose 5-phosphate (donor) and ribose 5-phosphate (acceptor) as substrates was used to investigate this proposed mechanism (Figure 10A). Incubation of stoichiometric amounts of tkt, TPP, and xylulose 5-phosphate afforded dihydroxyethylthiamine diphosphate (diHETP) (Figure 10B) (*30*). Stoichiometric amounts of tkt in these incubations were required to produce detectable amounts of diHETP, due to the extremely slow dissociation of diHETP from the enzyme. They also demonstrated that incubation of diHETP, ribose 5-phosphate, and stoichiometic amounts of tkt resulted in the formation of sedoheptulose 7-phosphate (*30*).

More recent studies by Schloss and co-workers investigated the kinetic mechanism of acetolactate synthase (*31*), which condenses two molecules of pyruvate to form acetolactate, or one molecule of pyruvate and one molecule of α-ketobutyrate to form acetohydroxybutyrate. In addition to these two physiological enzymatic reactions, acetolactate synthase catalyzes an oxygen-consuming side reaction, which has provided a useful tool for studying its mechanism. It was demonstrated that at low concentrations of pyruvate (below K_m), acetolactate synthase functions predominately

as an oxygenase, while higher concentrations of pyruvate or α-ketobutyrate inhibit the oxygenase reaction (*31*). It was suggested that this inhibition is due to the competition between molecular oxygen and pyruvate or α-ketobutyrate for the hydroxyethyl-TPP intermediate (*31*). On the basis of these results and additional experiments, it was concluded that decarboxylation of lactyl-TPP can occur prior to the binding of α-ketobutyrate or a second molecule of pyruvate (*31*).

Steady-state kinetic studies, inhibition studies, and CO_2 trapping experiments were used to investigate the kinetic mechanism of *R. capsulatus* DXP synthase. Initial velocity studies with varying concentrations of pyruvate and GAP provided double-reciprocal plots that were essentially parallel. The very small change in the slopes (<1%) is presumably due to a K_{ia} value that is very small compared to $K_m^{pyruvate}$ in an ordered mechanism. More specifically, the slopes are defined by eq 6 and the contribution of the $1 + K_{ia}/K_{mR}$ term is not significant. The analogous slopes in a ping-pong mechanism are defined simply by K_{mG}/V_{max}. A constant slope, similar to the observed slopes for the double-reciprocal plots, is predicted by the ping-pong rate equation. Therefore, the initial velocity data fit equally well to both the ordered and ping-pong rate equations.

Inhibition studies using a dead-end inhibitor that is competitive with respect to pyruvate were conducted in an attempt to resolve this ambiguity. An ordered mechanism predicts a noncompetitive pattern (changes in both the slopes and intercepts of the double-reciprocal plots) for β-fluoropyruvate when GAP is the varied substrate, whereas a ping-pong mechanism predicts an uncompetitive pattern (changes in only the intercepts). The slopes of these plots (Figure 6A) for an ordered mechanism are defined by eq 7.

$$\text{slope} = \frac{K_{mG}}{V_{max}}\left(1 + \frac{K_{ia}}{[R]} + \frac{K_{ia}[I]}{K_i[R]}\right) \qquad (7)$$

Again, under the conditions of the inhibition studies, the term in parentheses does not significantly contribute to the slopes, and therefore, the predicted and observed changes in the slopes are less than 10%. A similar trend for DXP synthase with pyruvate and D-glyceraldehyde as substrates was observed for both the initial velocity and inhibition studies.

A third set of experiments was conducted in an attempt to provide further evidence for an ordered mechanism. The results of the CO_2 trapping experiments demonstrated that DXP synthase does not efficiently catalyze the decarboxylation of pyruvate and release of CO_2 in the absence of GAP or D-glyceraldehyde. Therefore, the binding of GAP or D-glyceraldehyde is required for DXP synthase to form a catalytically competent complex.

On the basis of these results, an ordered mechanism can be proposed for DXP synthase, with pyruvate binding to the enzyme first followed by binding of GAP (Figure 11A). A similar ordered mechanism has been reported in the literature for PGGTase I, which catalyzes the condensation of an isoprenoid-derived C_{20} unit with a peptide substrate (*32*). Due to the small dissociation constant (K_{ia}) observed for the first substrate, double-reciprocal plots of the initial velocity data also showed a parallel pattern. When D-glyceraldehyde is the cosubstrate with pyruvate for DXP synthase, the results provide evidence for an ordered mechanism with substrate

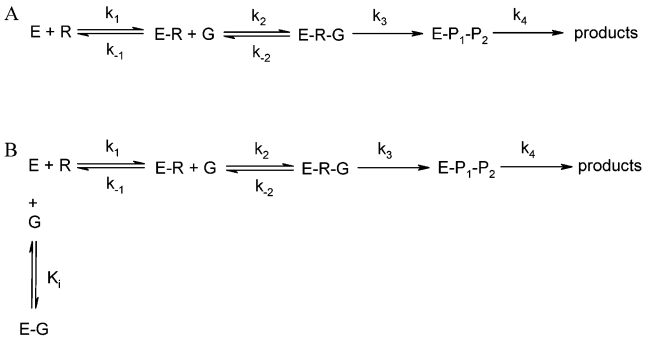

FIGURE 11: Kinetic mechanism for DXP synthase. (A) Ordered kinetic mechanism for DXP synthase with pyruvate (R) and GAP (G) as substrates. (B) Ordered kinetic mechanism with substrate inhibition for DXP synthase with pyruvate (R) and D-glyceraldehyde (G) as substrates.

inhibition by D-glyceraldehyde (Figure 11B). Substrate inhibition was also observed with PFTase, which catalyzes the condensation of a C_{15} isoprene moiety with a peptide substrate via an ordered mechanism (*33*). In conclusion, the proposed reaction mechanism for DXP synthase is consistent with PGGTase I and PFTase, which also catalyze condensation reactions involved in the isoprenoid biosynthetic pathway.

REFERENCES

1. Sacchettini, J. C., and Poulter, C. D. (1997) *Science 277*, 1788−1789.
2. Spurgeon, S. L., and Porter, J. W. (1981) in *Biosynthesis of Isoprenoid Compounds*, Wiley, New York.
3. Putra, S. R., Disch, A., Bravo, J.-M., and Rohmer, M. (1998) *FEMS Microbiol. Lett. 164*, 169−175.
4. Rohmer, M., Knani, M., Simonin, P., Sutter, B., and Sahm, H. (1993) *Biochem. J. 295*, 517−524.
5. Eisenreich, W., Schwarz, M., Cartayrade, A., Arigoni, D., Zenk, M. H., and Bacher, A. (1998) *Chem. Biol. 5*, R221−R233.
6. Rohmer, M. (1998) *Prog. Drug Res. 50*, 135−154.
7. Kuzuyama, T., Takahashi, S., Watanabe, H., and Seto, H. (1998) *Tetrahedron Lett. 39*, 4509−4512.
8. Takahashi, S., Kuzuyama, T., Watanabe, H., and Seto, H. (1998) *Proc. Natl. Acad. Sci. U.S.A. 95*, 9879−9884.
9. Himmeldirk, K., Kennedy, I. A., Hill, R. E., Sayer, B. G., and Spenser, I. A. (1996) *Chem. Commun.*, 1187−1188.
10. Rohdich, F., Wungsintaweekul, J., Fellermeier, M., Sagner, S., Herz, S., Kis, K., Eisinreich, W., Bacher, A., and Zenk, M. H. (1999) *Proc. Natl. Acad. Sci. U.S.A. 96*, 11758−11763.
11. Lüttgen, H., Rohdich, F., Herz, S., Wungsintaweekul, J., Hecht, S., Schuhr, C. A., Fellermeier, M., Sagner, S., Zenk, M. H., Bacher, A., and Eisenreich, W. (2000) *Proc. Natl. Acad. Sci. U.S.A. 97*, 1062−1067.
12. Herz, S., Wungsintaweekul, J., Schuhr, C. A., Hecht, S., Lüttgen, H., Sagner, S., Fellermeier, M., Eisenreich, W., Zenk, M. H., Bacher, A., and Rohdich, F. (2000) *Proc. Natl. Acad. Sci. U.S.A. 97*, 2486−2490.
13. Hecht, S., Wolfgang, E., Adam, P., Amslinger, S., Kis, K., Bacher, A., Arigoni, D., and Rohdich, F. (2001) *Proc. Natl. Acad. Sci. U.S.A. 98*, 14837−14842.
14. Rohdich, F., Hecht, S., Gärtner, A. P., Krieger, C., Amslinger, S., Arigoni, D., Bacher, A., and Eisenreich, W. (2002) *Proc. Natl. Acad. Sci. U.S.A. 99*, 1158−1163.
15. Sprenger, G. A., Schörken, U., Wiegert, T., Grolle, S., De Graaf, A. A., Taylor, S. V., Begley, T. P., Bringer-Meyer, S., and Sahm, H. (1997) *Proc. Natl. Acad. Sci. U.S.A. 94*, 12857−12862.
16. Bouvier, F., d'Harlingue, A., Suire, C., Backhaus, R. A., and Camara, B. (1998) *Plant Physiol. 117*, 1423−1431.
17. Kuzuyama, T., Takagi, M., Takahashi, S., and Seto, H. (2000) *J. Bacteriol. 182*, 891−897.
18. Hahn, F. M., Eubanks, L. M., Testa, C. A., Blagg, B. S. J., Baker, J. A., and Poulter, C. D. (2001) *J. Bacteriol. 183*, 1−11.

19. Schneider, G., and Lindqvist, Y. (1998) *Biochim. Biophys. Acta 1385*, 387−398.
20. Crout, D. H. G. (1990) in *Biosynthesis of Branched Chain Amino Acids*, pp 199−242, VCH, Weinheim, Germany.
21. Gubler, C. G. (1991) in *Biochemistry and Physiology of Thiamin Diphosphate Enzymes*, pp 311−321, Verlag Chemie, Weinheim, Germany.
22. Anderson, V. E., Weiss, P. M., and Cleland, W. W. (1984) *Biochemistry 23*, 2779−2786.
23. Bradford, M. M. (1976) *Anal. Biochem. 72*, 248−254.
24. Hess, H. H., and Derr, J. E. (1975) *Anal. Biochem. 63*, 607−613.
25. Touchstone, J. C., and Dobbins, M. F. (1978) in *Practice of Thin Layer Chromatography*, p 182, Wiley, New York.
26. Leatherbarrow, R. J. (1992) *Grafit*, version 3.01, Erithacus Software Ltd., Staines, England.
27. Fujisawa, H., and Okuno, S. (1987) *Methods Enzymol. 142*, 63−71.
28. Segel, I. H. (1975) in *Enzyme Kinetics*, pp 564−565, Wiley, New York.
29. Laskovics, M. F., Krafcik, J. M., and Poulter, C. D. (1979) *J. Biol. Chem. 254*, 9458−9463.
30. Krampitz, L. O. (1969) *Annu. Rev. Biochem. 38*, 213−240.
31. Tse, J. M.-T., and Schloss, J. V. (1993) *Biochemistry 32*, 10398−10403.
32. Stirtan, W. G., and Poulter, C. D. (1997) *Biochemistry 36*, 4552−4557.
33. Dolence, J. M., Cassidy, P. B., Mathis, J. R., and Poulter, C. D. (1995) *Biochemistry 34*, 16687−16694.

BI0205303